Journal of Molecular Catalysis A: Chemical 408 (2015) 75–84

Contents lists available at ScienceDirect

Journal of Molecular Catalysis A: Chemical

journal homepage: www.elsevier.com/locate/molcata

In situ FTIR and Raman study on the distribution and reactivity of surface vanadia species in V_2O_5/CeO_2 catalysts

Marta V. Bosco[a], Miguel A. Bañares[b], María V. Martínez-Huerta[b], Adrian L. Bonivardi[a], Sebastián E. Collins[a,*]

[a] Instituto de Desarrollo Tecnológico para la Industria Química (INTEC) UNL-CONICET, Güemes 3450, 3000, Santa Fe, Argentina
[b] Instituto de Catálisis y Petroleoquímica, CSIC, Campus Cantoblanco, E-28049 Madrid, Spain

ARTICLE INFO

Article history:
Received 24 April 2015
Received in revised form 9 July 2015
Accepted 10 July 2015
Available online 17 July 2015

Keywords:
Vanadia
Ceria
Methanol oxidation
Raman
Infrared spectroscopy

ABSTRACT

The surface structure and reactivity of vanadia supported on ceria catalysts were studied by Raman spectroscopy and methanol adsorption and temperature-programmed surface reaction (TPRS) of the adsorbed species monitored in situ by infrared spectroscopy. Monomeric and polymeric vanadia surface species and $CeVO_4$ were identified on the catalysts. Methanol adsorption reveled that mostly reduced Ce^{3+} sites are present in the surface of the catalysts, produced as a result of the reductive solid reaction of VO_x species with the ceria surface. Adsorbed methanol/methoxy decomposed stepwise to formate and, finally, carbonate/carbon dioxide. The reactivity is linked to interphase sites, Ce–O–V, which could favor the abstraction of hydrogen during the methoxy transformation to formates.

1. Introduction

Catalysts based on supported vanadium oxide are among the most active and selective for partial oxidation reactions [1] and oxidative dehydrogenation (ODH) of alkanes [2], either in the gas or liquid phase. The performance of these catalysts strongly depends on the chosen support and surface structures formed by vanadium. Among all supports for vanadia, ceria has shown particularly high turnover frequency values per vanadium site for methanol oxidation [3–7], which makes it a very special system. Although, several works have been devoted to understand the structure/reactivity relationship in vanadia-ceria catalysts, the role of surface V=O, bridging V—O—V or the bridging V—O—support sites is still matter of debate [8–14].

Raman spectroscopy is a widely used characterization technique because it can provide fundamental information about molecular structures of surface sites [14]. Particularly, Raman was employed to identify surface vanadia species due to the fingerprint signals of these groups. Some of us [15] investigated ethane ODH over ceria-supported vanadium oxide by operando Raman-GC. Surface vanadia species have a marked influence on the structure and reactivity of the Ce sites at its interface. The presence of surface VO_x species, which react with the support forming $CeVO_4$ were detected and correlated with the functionality of the active site, V—O—Ce bonds, present in both systems, e.g., VO_x/CeO_2 and $CeVO_4/CeO_2$.

The chemisorption of probe molecules is a well-known method to characterize the surface of catalytic materials. Particularly, the chemisorption of methanol has proven to be a reliable method for determining the nature and number of active sites, as well as can supply essential data from the decomposition temperature of surface methoxy intermediates on metal oxide catalysts [1,16]. Thus, Badlani and Wachs demonstrated that methanol chemisorbs at 373 K, forming a stable monolayer of methoxy species (CH_3O-) [1]. Finocchio et al. [17] and Binet et al. [18] reported that methoxy species with different surface coordination on Ce^{3+} or Ce^{4+} cations can be identified by means of their characteristic infrared signals, ν(CO).

In this work the distribution and reactivity of surface species on V_2O_5/CeO_2 catalysts, and reference materials CeO_2 and $CeVO_4$, are investigated by means of in situ Raman spectroscopy and methanol chemisorption and temperature-programmed surface reaction (TPSR) followed by in situ infrared spectroscopy.

2. Experimental

V_2O_5/CeO_2 materials were prepared by wetness impregnation with vanadium triisopropoxide in a glove box under nitrogen flow on pure CeO_2 (Engelhard, 40 m^2/g) as reported elsewhere [15,19].

* Corresponding author.
E-mail address: scollins@santafe-conicet.gov.ar (S.E. Collins).

http://dx.doi.org/10.1016/j.molcata.2015.07.012
1381-1169/

The catalysts are referred to as *x*VCe, where *x* represents the weight percent of V_2O_5 on CeO_2. $CeVO_4$ was provided by Alfa (99.9%, 45 m^2/g).

2.1. Raman spectroscopy

Raman spectra were collected using a Renishaw System 1000 spectrometer equipped with an Ar laser (514.5 nm), a cryogenic CCD detector (200 K) and Edge type filter. The spectral resolution was 3 cm^{-1}. The samples were in powder form and were located in an in situ cell (Linkam, TS-1500), which allow thermal treatment in flow of gases. Raman spectra were acquired after activation pretreatment, consisting in a calcination under O_2 (5%)/He (50 cm^3/min) up to 723 K, followed by purge with pure He (50 cm^3/min) and cooling to room temperature.

2.2. In situ infrared spectroscopy

The methanol adsorption and temperature programmed surface reaction (TPSR) of the adsorbed species were followed by in situ infrared Fourier transform spectroscopy (FTIR). Self-supporting wafers of each material (30 mg, d = 13 mm) were placed in a heated cell fitted with NaCl windows, which was attached to a conventional high vacuum system, equipped with a manifold for gas flow operation described elsewhere [20]. Spectra were recorded in transmittance mode using a Nicolet 8700 FTIR spectrophotometer equipped with a MCT detector.

Before the chemisorption of methanol, each wafer was subjected to the following in situ pretreatment in order to clean the surface of the sample: (i) heating (10 K/min) under flow of H_2 (50 cm^3/min) from room temperature to 723 K (15 min), (ii) purging with He (50 cm^3/min, 15 min), followed by oxidation under pure O_2 flow (50 cm^3/min, 15 min) at the same temperature, (iii) cooling under flowing O_2 to 373 K, and finally, (iv) the cell was swept with He flow (60 cm^3/min, 15 min). Reference IR spectra of the "clean wafer" were taken at different temperatures (every 25 K) under O_2 flow. Next, the sample was exposed to a stream containing 5% v/v of CH_3OH in He at 25 cm^3/min flow for 15 min to allow saturation of the surface. Once saturated, the cell was purged again under He flow (50 cm^3/min, 15 min) and a temperature programmed surface reaction (TPSR) experiment was performed by heating the IR cell from 323 to 723 K at 5 K/min always under He flow (60 cm^3/min). Along the temperature ramp, IR spectra were acquired every 30 s, averaging 25 scans, at a resolution of 4 cm^{-1}. When it was necessary, background correction of the spectra was achieved by subtracting the spectra of the pretreated cleaned wafer at each temperature; Lorentzian sum function were used to fit the overlapped bands and to measure peak areas and/or intensities.

Methanol (Merck, 99.9%) was supplied to the system by a saturator located in a thermostatic bath, in order to send, via a 4 ways valve, a fixed concentration of vaporized methanol. All the gases used in this work were high purity grade (99.999%) and were further purified as mentioned in previous work [21].

3. Results and discussion

3.1. Characterization and in situ Raman

The surface area of CeO_2 was 40 m^2/g, and decrease after impregnation with vanadia to 30 and 15 m^2/g for 2VCe and 5VCe, respectively (see Supplementary information). A high degree of dispersion of vanadium oxide species was reported previously by X-ray phtotelectron spectroscopy (XPS) [15].

Fig. 1 shows the in situ Raman spectra of each activated material dehydrated in situ under He flow at 573 K (15 min). For comparison proposes, the Raman spectrum of pure V_2O_5 is also included in

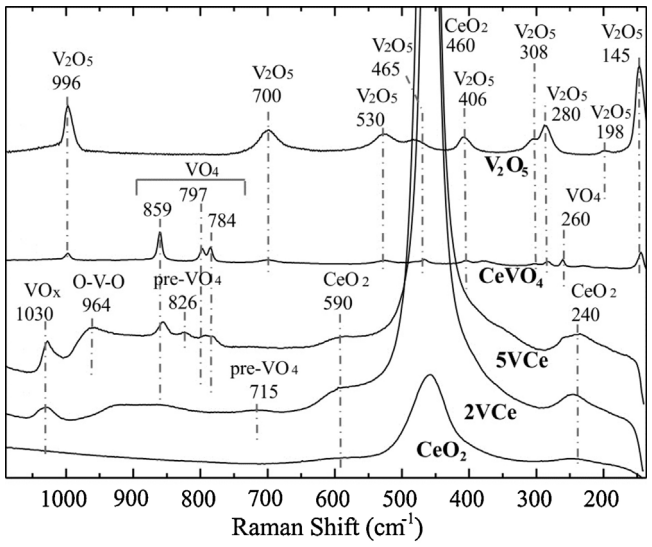

Fig. 1. In situ Raman spectra of activated dehydrated CeO_2, 2VCe, 5VCe, $CeVO_4$ catalysts. (V_2O_5 is included for comparison proporses).

Fig. 1. Additionally, Raman spectra were taken after methanol TPSR-IR runs and similar spectra were obtained (not shown). Pure ceria presents the characteristic band at 460 cm^{-1} assigned to the F_{2g} mode of fluorite type cubic structure corresponding to the symmetric vibration of oxygen ions around Ce^{4+} ions in the CeO_6 octahedral. Also a couple of weak bands are observed at 590 and 240 cm^{-1}, due to second-order scattering tensors A_{1g}, E_g and F_{2g} [22,23].

The reference $CeVO_4$ material presents a series of characteristic sharp bands at 860, 797, 786 and 260 cm^{-1} which are assigned to this crystalline material [24]. Additionally, peaks due to segregated V_2O_5 crystals are observed at 996, 280 and 145 cm^{-1} [7,25–28]. A very small signal at 465 cm^{-1} is assigned to assigned to the B_{2u} [δ (V—O—V)] mode of V_2O_5 as well as the bands at 380, 406, 526 and 700 assigned to V—O—V modes [25,28]. The very weak mode near 465 cm^{-1} may also be due to some traces of unreacted CeO_2 in $CeVO_4$, whose characteristic mode is located at 460 cm^{-1}.

In the case of both 2VCe and 5VCe catalysts, in addition to the CeO_2 features, Raman signals associated with surface vanadium species are present at 1028 cm^{-1}. This latest signal is characteristic of the V=O stretching mode of dehydrated, molecularly dispersed, vanadium oxide species (VO_x) on ceria [15,25,26,28]. Additionally, a broad band is registered at 964 cm^{-1}, more noticeable in the higher loading catalyst, which can be assigned to V—O—V vibrations in surface polymeric $(VO_x)_n$ species [15]. 2VCe sample also presents a feature at 715 cm^{-1}, which could be ascribed to the V—O—Ce stretching mode, similar to a precursor cerium vanadate species, as proposed previously [15,29]. 5VCe catalyst shows bands at 859, 797, 784 and 260 cm^{-1} characteristic of $CeVO_4$, formed by solid–solid reaction at the surface of the ceria during the reduction step of the pretreatment. Finally, there is no evidence of crystals of V_2O_5, which presents several strong Raman bands, in any of the dispersed vanadia catalysts [8,15,25,26]. Table 1 summarizes the Raman signals registered on each sample and their assignation.

To summarize, results from the Raman analysis indicates that 2VCe is composed essentially of surface monomeric VO_x species and, what can be thought as, a precursor of cerium vanadate along with some polymeric VO_x species.

3.2. Surface species after methanol adsorption at 373 K

The adsorption of methanol on the investigated samples was carried out at 373 K in order to generate a stable monolayer of

Table 1
Assignment of Raman signals registered on CeO_2, $CeVO_4$, V_2O_5, 2VCe and 5VCe samples.

Mode	CeO_2	2VCe	5VCe	$CeVO_4$	V_2O_5	Reference
	Wavenumber (cm^{-1})					
B_{2g} [δ (O=V—O)]				145	145	[25,28]
A_g [δ (V—O—V)]					198	[25,28]
$A_{1g} + E_g + F_{2g}$ [ν (Ce—O)]	240	245	237			[22]
B_{3g} [δ (V—O—V)]			260	260		[15,25,26]
B_{3g} [δ (O=V—O)]				280	280	[7,24,25,28]
B_{1g} [δ (V—O—V)]					308	[7,25,28]
$A_{1g} + B_{1g}$ [δ (V—O—V)]				380		[15,24–26]
A_g [δ (V—O—V)]				406	406	[7,24,25,28]
F_{2g} [ν (Ce—O)]	460	460	460	465		[22,24]
B_{2u} [δ (V-O-V)]				465[a]	468	[7,25,28]
A_g [ν (V—O—V)]				526	528	[7,25,28]
$A_{1g} + E_g + F_{2g}$ [ν (Ce—O)]	590	590	590			[22]
B_{2g} [ν (V—O—V)]				700	700	[7,25,28]
[ν (V—O—Ce)]		715				[15]
E_g [ν_{as} (V—O—V)]			784	786		[15,24,26]
B_{2g} [ν_{as} (V—O—V)]			797	797		[24]
[ν (V—O—Ce)]			826			
A_{1g} [ν_s (V—O—V)]			859	859		[15,24]
B_{1g} [ν_{as} (V=O)]		964				[15,25,28]
A_g [ν_s (V=O)]				996	996	[7,24,25,28]
$A_g + B_{1g}$ [ν_s (V=O)]		1030	1028			[15,25,26,28]

[a] May also be due to some traces of unreacted CeO_2 in $CeVO_4$, which characteristic mode is at 460 cm^{-1}.

chemisorbed methoxy species. Previous studies proved that mostly molecularly adsorbed methanol species are formed at lower temperatures and that further decomposition of methoxy species demand higher temperatures [30–32].

Upon exposing each catalyst to a flow of 5% v/v of CH_3OH in He for 15 min, the saturation of the surface was reached, that is, stationary IR signals were registered. Next, the IR cell was flushed with pure He in order to eliminate weakly adsorbed species. Fig. 2 shows the IR spectra obtained for each sample after methanol adsorption at 373 K. Background corrections of the spectra were achieved by subtracting the corresponding spectra of the pre-treated cleaned wafer at the same temperature, except for the 1200–900 cm^{-1} region, for the sake of clarity, as will be discussed next.

The consumption of OH signals is evidenced in Fig. 2, illustrated by negative bands between 3750 and 3580 cm^{-1}. These negative signals indicate the loss of the surface OH groups upon methanol adsorption and dehydration at 373 K as demonstrated in previous works [16,20].

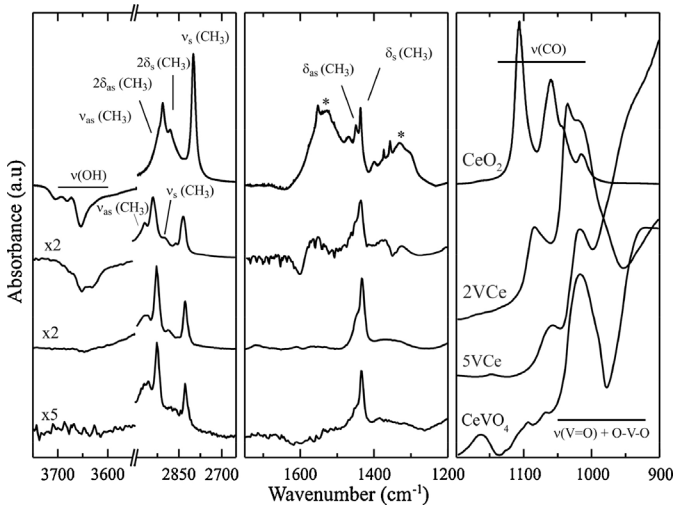

Fig. 2. IR spectra after CH_3OH adsorption at 373 K on CeO_2, 2VCe, 5VCe and $CeVO_4$. *Residual carbonates.

IR absorption bands due to molecularly adsorbed methanol (CH_3OH_S) and methoxy (CH_3O) species develop in the 3000–2800 cm^{-1} region: (i) overtone of the symmetric and asymmetric C—H bending vibration, strongly perturbed by Femi resonance, $2\delta_s(CH_3)$ at 2885–2896 cm^{-1}, and $2\delta_{as}(CH_3)$ at 2910–2930 cm^{-1}, respectively and (ii) symmetric and asymmetric CH_3 stretching, $\nu_s(CH_3)$ at 2805–2830 cm^{-1}, and [$\nu_{as}(CH_3)$] at 2940–2985 cm^{-1}, respectively [20,33,34]. Noteworth that this spectral region is quite controversial because some authors have attributed the most intense couple of peaks (that is, the ones centered at ~2950 and ~2850 cm^{-1}) to the asymmetric and symmetric stretching modes of methoxy groups, $\nu_{as}(CH_3)$ and $\nu_s(CH_3)$, respectively [4,35–38]. In any case, these signals are mostly similar among the catalysts, due to their poor sensitivity to the surface coordination of the adsorbed groups. Consequently, this spectra region is not appropriated to perform a detailed identification of surface species.

In the 1600–1200 cm^{-1} region, symmetric bending C—H modes of both CH_3OH_S and CH_3O groups were observed around 1435 [$\delta_s(CH_3)$] for the four materials, while the signal of the asymmetric bending mode [$\delta_{as}(CH_3)$] at 1467 cm^{-1}, is observed only for CeO_2. Features due to remaining carbonates groups are observed only in the pure CeO_2 sample.

The IR spectra in the C—O stretching zone (1250–950 cm^{-1}) allow a fingerprint identification of the different methanol/metoxy species and a correlation with the oxidation state of ceria sites [18,20]. However, in this region IR signals from vanadia surface species are also present, which complicate the analysis of the individual peaks. Fig. 3 shows in more detail the IR spectra before and after the adsorption of methanol, and the subtracted spectrum, for each sample. The IR spectra collected on the vanadia-supported catalysts present signals at 1040 and 1023 cm^{-1} in 2VCe, and at 1034 and 1019 cm^{-1} in 5VCe, which are ascribed to the stretching vibrations of V=O (vanadyl) with different symmetries and degrees of polymerization [9,13,37,39,40]. The bridging, V—O—V mode, from polymerized surface vanadia species is also observed as a broad band at ~998 cm^{-1} in 2VCe, at ~1013 cm^{-1} in 5VCe. Moreover, IR bands due to the overtone of the V=O mode is registered at 1900–2100 cm^{-1} [9] (see Fig. S1 in the Supplementary information). This frequency is approximately twice the fundamental frequency, which indicates some anharmonicity in the V=O mode, and corroborates the assignment of V=O modes [39,41,42].

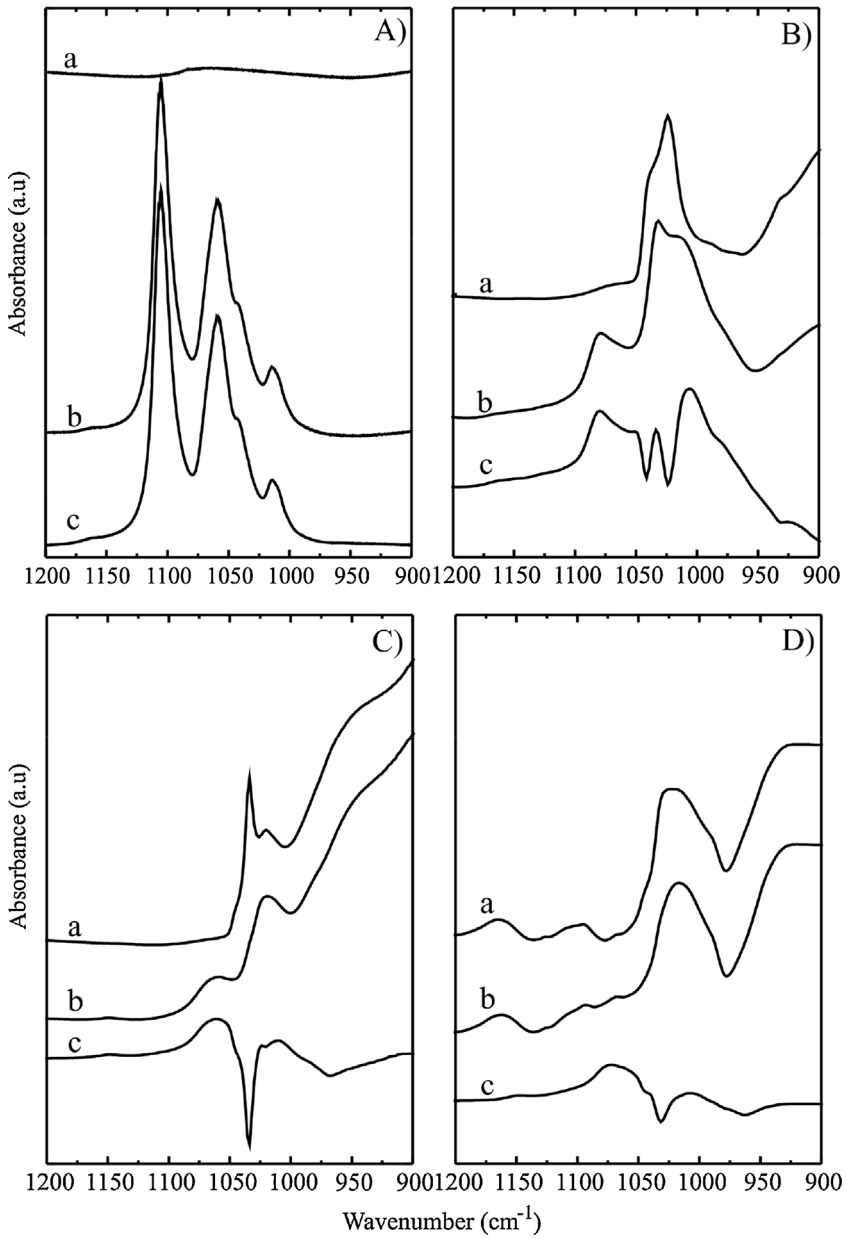

Fig. 3. IR spectra in the C—O stretching zone (1250–950 cm^{-1}) for (A) CeO_2, (B) 2VCe, (C) 5VCe and (D) $CeVO_4$. Spectra are labeled as follows: (a) clean catalysts before chemisorptions of methanol; (b) catalyst after chemisorption of methanol at 373 K; (c) difference spectrum, (b)–(a).

In the case of $CeVO_4$, a broad band is registered between 1050 and 975 cm^{-1}. Some authors assigned this IR bands to phonon modes of the solid, e.g., in $TlVO_4$ [43] and $CeVO_4$ [24]. Additionally, part of this band possess contribution from surface vanadyl group due to defects in the solid [14], as corroborated by the presence of the overtone signal described before.

After methanol adsorption, all those bands are affected in some degree, decreasing their intensity and shifting their position (Fig. 3 and Fig. S1). As highlighted in the difference spectra, a perturbation of the vanadyl bands generates negative and shifted peaks, which complicate the analysis of the signals due to methanol/methoxy species. This observation is a clear evidence of the interaction of methanol with vanadium surface sites as was also predicted by molecular modeling of the methanol chemisorption on VO_x/CeO_2(1 1 1) [10]. According to Kropp et al. [10] the partial extinction of the V=O stretching band upon methanol adsorption is due to three effects: (i) interaction with the CH_3O dipole, (ii) tilting of V=O toward the surface (selection rule), and (iii) screening of the V=O dipole by the OH dipoles.

To assess the distribution of methanol/methoxy surface species, Fig. 4 shows the deconvolution of each IR peak, including those belonging to V=O species. The signals already present before the methanol chemisorption are displayed in this last figure by dash lines, which represent the best fitting of the spectra after taking into account both: decreasing and shifting of the vanadyl bands after methanol chemisorption. In the case of pure CeO_2, signals are present at 1106, 1054 and 1013 cm^{-1} corresponding to methoxy species (CH_3O): mono- (type-I), di- (type-II) and tri- (type-III) coordinated on Ce^{4+} sites, respectively; and at 1038 cm^{-1} of molecularly adsorbed methanol (CH_3OH_S) as was reported by several authors [11–18,20,44–51]. Conversely, $CeVO_4$ shows a very different distribution of IR bands. After methanol adsorption, a broad band at 1008 cm^{-1} rose, which is assigned to methoxy species on vanadium sites of the $CeVO_4$ [41,52]. Furthermore, a weak signal at 1074 cm^{-1}

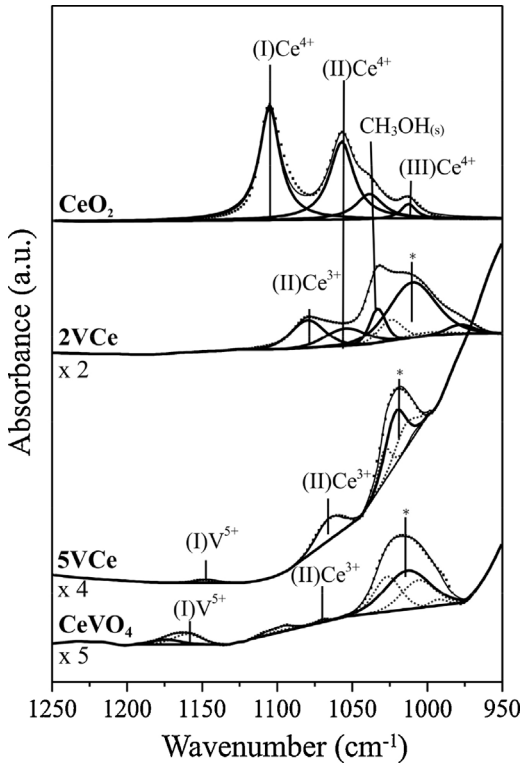

Fig. 4. Resolved IR signals for CH_3OH_S and CH_3O surface species on ceria and vanadia sites (solid bold lines). Dotted lines represent the IR signals from the catalyst already present before the methanol adsorption. * Band assigned to CH_3O species bonded to $CeVO_4$.

is ascribed to CH_3O type-II on Ce^{+3}, and a peak at 1150 cm^{-1} is associated with CH_3O on V^{+5} sites on segregated V_2O_5 crystals. This is consistent with Raman observation of vanadia nanocrystals.

After methanol adsorption on 2VCe and 5VCe catalysts, the intensity of the signals were 2.5–15-fold weaker than in pure ceria. The most remarkable observation is the total loss of the band at 1106 cm^{-1} from methoxy type-I species on Ce^{4+} sites. At the same time, new signals that could be ascribed to methoxy species on reduced Ce^{3+} sites develop. In the 2VCe sample a new signal is observed at 1080 cm^{-1}, which is assigned to type-II methoxy groups on Ce^{3+} cations [18]. Additionally, the peak at 1055 cm^{-1} due to type-II species on Ce^{4+} remains, but with a lower intensity. Likewise, the 5VCe catalyst presents a band at 1066 cm^{-1} also assigned methoxy type-II on Ce^{3+} and, in this case, a band at 1150 cm^{-1} ascribed to methoxy species adsorbed on vanadium sites (CH_3O–V). Only on 2VCe the band of molecularly adsorbed methanol was observed at 1032 cm^{-1}. Furthermore, a weak band could be recognized in both catalysts at ca. 1005 cm^{-1}, partially overlapped with the signals of the solid, which could be assigned to CH_3O type-III on Ce^{3+}, or methoxy species on cerium vanadate. The resulting assignment of each IR band to the corresponding vibrational modes is summarized in Table 2.

Altogether, the incorporation of vanadium decreases the formation of surface methoxy species, and particularly inhibits the formation type-I CH_3O groups on Ce^{4+}. Thus, methanol adsorption reveals the presence of surface Ce^{3+} sites, in spite of the oxidative pretreatment applied to each sample.

3.3. Temperature-programmed surface reaction of adsorbed methanol

The thermal evolution of adsorbed species was followed by temperature-programmed surface reaction experiments monitored by in situ IR spectroscopy (TPSR-IR). Figs. 5–8 show the IR spectra during the TPSR-IR, between 373 and 723 K. Characteristic IR bands for each surface species was used to follow their concentration along the temperature ramp, as Fig. 9 illustrates.

On CeO_2, the concentration of CH_3OH_S species decreased quickly during TPSR, vanishing near 470 K. CH_3O groups, type-I–III, present different thermal stability. When heated, the concentration of type-I methoxy species gradually decrease, until showing a negligible signal near 553 K. Dicoordinated methoxy (type-II) species are stable up to 573 K. Type-III remains essentially constant until 523 K and finally sharply decrease at 573 K. Thus, mono- (type-I) and dicoordinated(type-II) methoxy species are less stable and more reactive than type-III species on the ceria surface, which is in agreement with previous reports on ceria based catalysts [49,50].

Then, from 473 K onwards, a set of bands emerge in the 3000–2700 cm^{-1} and 1650–1300 cm^{-1} regions, which are characteristic of formate groups with different surface coordination, as was reported over a diversity of metal oxides and in organometallic complexes [17,20,44,49,50,53,]. According to their bands position and band-separation of the asymmetric and symmetric OCO stretching modes [$\Delta\nu(OCO) = \nu_{as}(OCO) - \nu_s(OCO)$], formate species can be distinguished [44,55]. Fig. S2 and Table S2 show details of the IR bands from each formate species on ceria, which are ascribed to monodentate (m-HCOO), two types of bidendetate (b-HCOO and b'-HCOO) and bridged (br-HCOO) groups [17,44,49,50,53,55–59]. It was observed that bridged formate (br-HCOO) rise from 473 K, reached a maximum at 523 K and then decreased to disappear at 573 K. Mono- and bidentate formates followed a similar thermal evolution, from 498 K, reaching a maximum at 573 K, and vanishing at 623 K. At temperatures higher that 600 K, a set of bands rises in the region of 1500–1300 cm^{-1} (Fig. 6). These bands correspond to carbonate groups [54,60–64], which accumulate on the ceria surface after the decomposition of the formate groups. The evolution of the integrated band $\nu_{as}(OCO)$ of the whole set of formate groups on ceria is presented in Fig. 9 (a).

The TPSR on $CeVO_4$ (Figs. 6 and 9d), shows that methoxy species decayed in concentration to vanish at 473 K. Formate groups (b-HCOO, b'-HCOO and br-HCOO) are also observed, emerging at 448 K, reached a maximum at 523 K and vanished at 573 K. No traces of carbonate groups could be registered. At the same time, negative bands due to hydroxyl groups recovered during the temperature ramp for CeO_2, 2VCe and 5VCe. In the case of $CeVO_4$ the evolution of the OH bands is not observed due to the low coverage of OH groups (Fig. 6).

Methanol adsorption on ceria-supported vanadia catalyst forms CH_3O type-II and -III on Ce^{3+}, and methoxy on vanadia. During the temperature ramp, all methoxy groups decayed at a similar rate, disappearing at lower temperature on the 5VCe catalyst (473 K) that on 2VCe (523 K) (Figs. 7 and 8). Note here that bands remaining in the 1100–1000 cm^{-1} region at temperature higher than 473 K belong to V=O as indicated above. At 425 K, characteristics signals of formate groups showed up (Figs. 7–9 b and Fig. 99d). Results show that the reactivity of formate groups follows the following order: 5VCe > $CeVO_4$ > 2VCe > CeO_2, that is, higher reactivity of formate groups was observed in the presence of vanadia surface species. Conversely to the results from pure ceria, there are no traces of surface carbonate species. Finally, it is worth noticing that during the TPRS, an increase of the signal at 2130 cm^{-1} was registered. This band is assigned to the forbidden electronic transition $^2F_{5/2}$–$^2F_{7/2}$ of Ce^{3+} in surface or sub-surface sites [18,65]. As shown in Fig. S3 for both 2VCe and 5VCe catalysts, this band increased after decomposition of methoxy and formates. This result indicates that there is a reduction of other ceria sites at the interface with vanadia, and such reduction is related with the oxidation of methanol to CO_2. As was stated before, the reduction of additional cerium ions

Table 2
IR bands assignment to adsorbed methanol and methoxy groups.

Mode	CeO_2 Wavenumber (cm^{-1})	2VCe	5VCe	$CeVO_4$
ν_{as} V—O—V		998	1013	995
ν V=O terminal isolated		1023	1019	1005
ν V=O terminal in polymerized		1040	1043	1025
ν (CO) -CH_3O (Ce-III)	1013			
Ce—V—CH_3O		1010	1010	1008
ν (CO) CH_3OH_s	1038	1032 (ov)		
ν (CO) -CH_3O (Ce-II)	1054 → 1035	1055 (Ce^{4+})	1066 (Ce^{3+})	1074 (Ce^{3+})
		1080 (Ce^{3+})		
ν (CO) -CH_3O (Ce-I)	1106 → 1089			
ν (CO) -CH_3O (V^{5+})		1150 (vw)	1150	1150
δ_s (CH) CH_3OH + -CH_3O	1436	1434	1432	1436
δ_{as} (CH) CH_3OH + -CH_3O	1467			
ν_s (CH_3) -CH_3O	2805 → 2807	2826	2828	2828
ν_s (CH_3) CH_3O—V		2884	2882	
$2\delta_s$(CH_3) CH_3OH + -CH_3O	2886	2889	2887	2896
$2\delta_{as}$(CH_3) -CH_3O	2912	2928	2927	2925
ν_{as} (CH_3) CH_3O—V		2959	2965	2963
ν_{as} (CH_3) -CH_3O	2943 (sh)	2985 (sh)	2974	2981

(vw) Very weak; (br) broad; (sh) shoulder; (ov) overlapped.

at the interface of V-Ce sites was demonstrated by experimental data [67] and explained by computational chemistry [39].

4. Discussion

The structure of ceria, cerium vanadate and ceria-supported vanadia was investigated by in situ Raman spectroscopy. Monomeric and polymeric VO_x species co-exist on 2VCe and 5VCe along with $CeVO_4$ in the catalyst with the highest vanadia loading. Whereas, in 2VCe a signal of a precursor of $CeVO_4$ at 715 cm^{-1} was registered (Fig. 1).

Methanol was used as a surface sensitive probe molecule to characterize the structure and reactivity of these catalytic materials. The adsorption of methanol on pure CeO_2 produced the usual distribution of methoxy groups in type-I–III on the pre-oxidized solid (i.e., on Ce^{4+}) [16–18,20,44–51] (Fig. 4). Conversely, methoxy species bonded to Ce^{3+} and to V^{5+} were identified on $CeVO_4$ (Fig. 4). Noteworthy, vanadia dispersed on ceria inhibits the formation of methoxy type-I species on Ce^{4+} and only a small signal of methoxy type-II on Ce^{4+} could be registered on 2VCe. Instead, bridged type-II methoxy species on Ce^{3+} sites were observed (Fig. 4). As reported by Binet et al. [18], when ceria is reduced the bands assigned to methoxy type-II and -III blue-shift along with the vanishing of the methoxy type-I signal. These results clearly indicate that most of the ceria adsorption sites are reduced in 2VCe and 5VCe catalysts, regardless of the oxidative pretreatment.

As reported before, the interaction between vanadia and ceria is particularly intense and unique; there is a strong reductive inter-

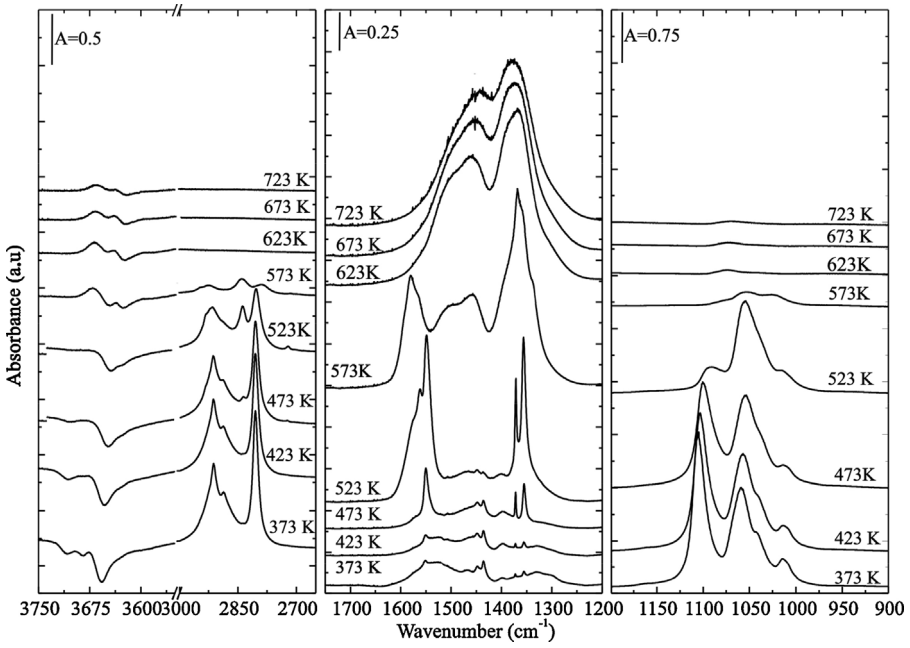

Fig. 5. IR spectra during the temperature-programmed surface reaction (TPSR) of adsorbed methanol on CeO_2.

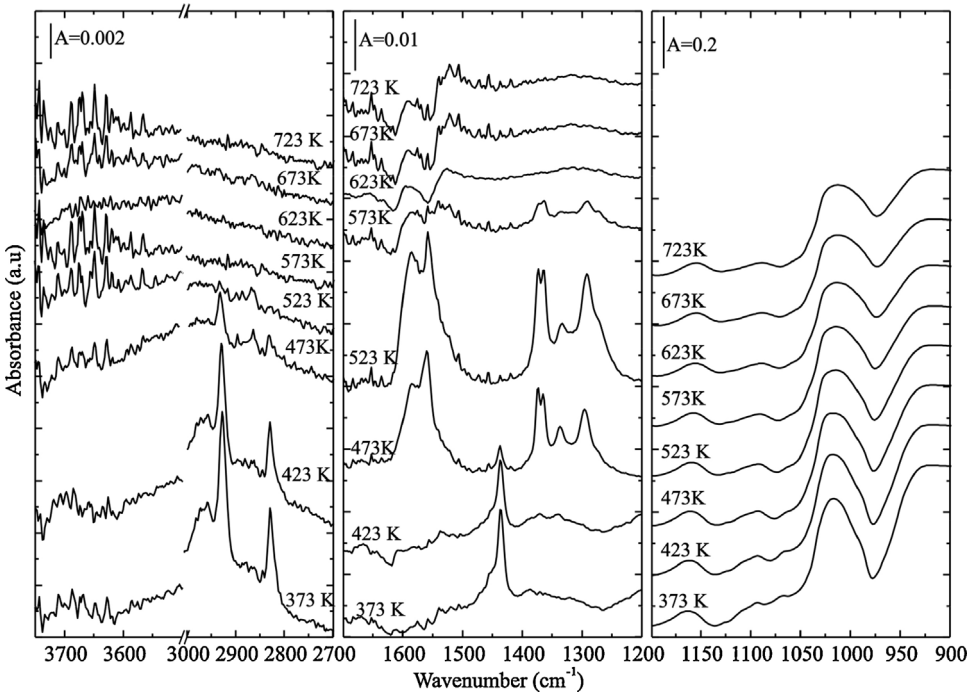

Fig. 6. IR spectra during the temperature-programmed surface reaction (TPSR) of adsorbed methanol on $CeVO_4$.

action that tends to form $CeVO_4$, even in oxidizing conditions [15,66,67]. The formation of $CeVO_4$ is favored in reducing environment, as shown by TPR-Raman [10] and during redox catalytic operation, as shown by operando Raman-GC [61]. The unique feature of vanadia-ceria interface is that ceria sites at the interface tend to reduce, stabilizing vanadium as 5+, to the point it cannot be reduced, at least up to 800 °C [67]. XPS and EPR results confirmed the absence of reduced vanadia and the presence of surface Ce^{3+} ions [15,24,66,67].

Hence, the identification by Raman of $CeVO_4$ phase and the above results obtained by methanol adsorption confirm the reductive reaction of surface CeO_2 with dispersed VO_x species: $Ce^{4+}O_2 + VO_x \rightarrow Ce^{3+}VO_4$. Thus, the presence of vanadia dispersed on the surface of the ceria, results in a very strong preference to form V^{5+}–Ce^{3+} oxide phases, where vanadium remains as 5+, but Ce is reduced, as was shown before by Martinez-Huerta et al. [2,15].

Very recently, Kropp et al. [10] investigated by means of DFT calculations, the chemisorption of methanol on a model VO_x/CeO_2(1 1 1). Two adsorption sites were identified one on the vanadium atom (V^{5+}) and other in the V–O–Ce^{3+} interphase. This model is in good agreement with the experimental results presented here.

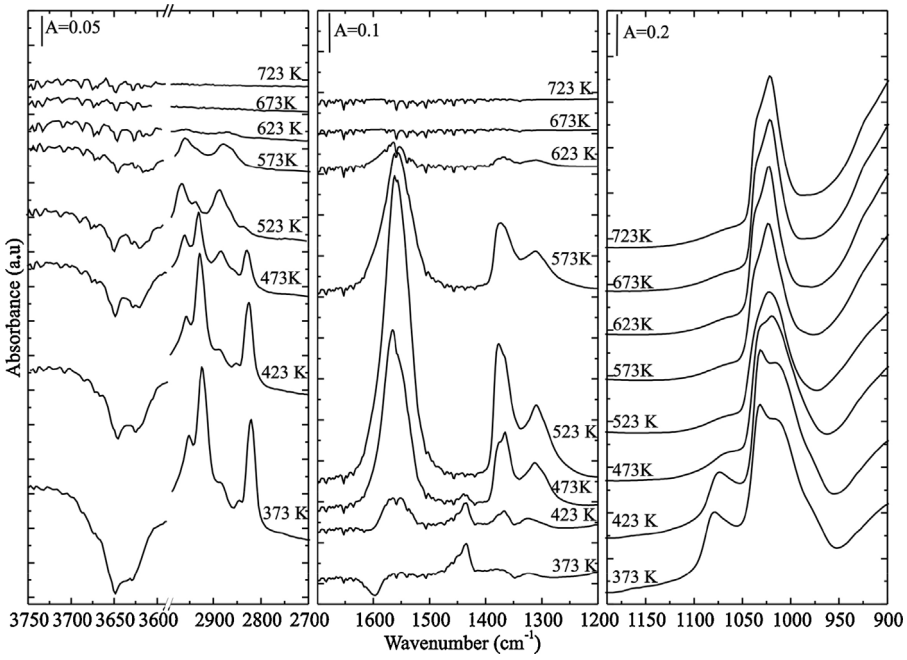

Fig. 7. IR spectra during the temperature-programmed surface reaction (TPSR) of adsorbed methanol on 2VCe.

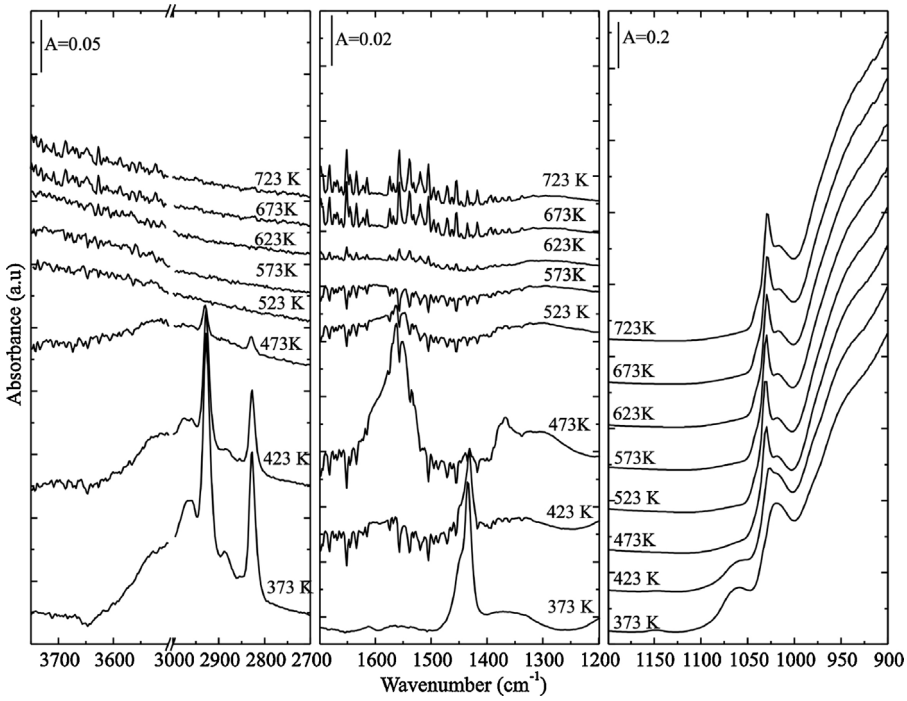

Fig. 8. IR spectra during the temperature-programmed surface reaction (TPSR) of adsorbed methanol on 5VCe.

Methanol TPSR-IR allows studying the relationship between structure and reactivity on these materials upon interaction with methanol/methoxy species. The stability of these surface species follows the order: CeO_2 > 2VCe > $CeVO_4$ > > 5VCe, indicating that the presence of vanadia surface species enhances oxidation activity of the catalysts (Fig. 9). Methoxy species stepwise decompose upon heating producing formate species (with different surface coordinations); these in turn decompose into $CO_3^=$ (e.g., adsorbed CO_2). Note that the carbonate groups produced by the adsorption of carbon oxides, were observed only on the (basic) surface of CeO_2 but not on the VCe or $CeVO_4$ samples. This is indicative that acidic vanadia sites "titrate" the most reactive basic sites of ceria.

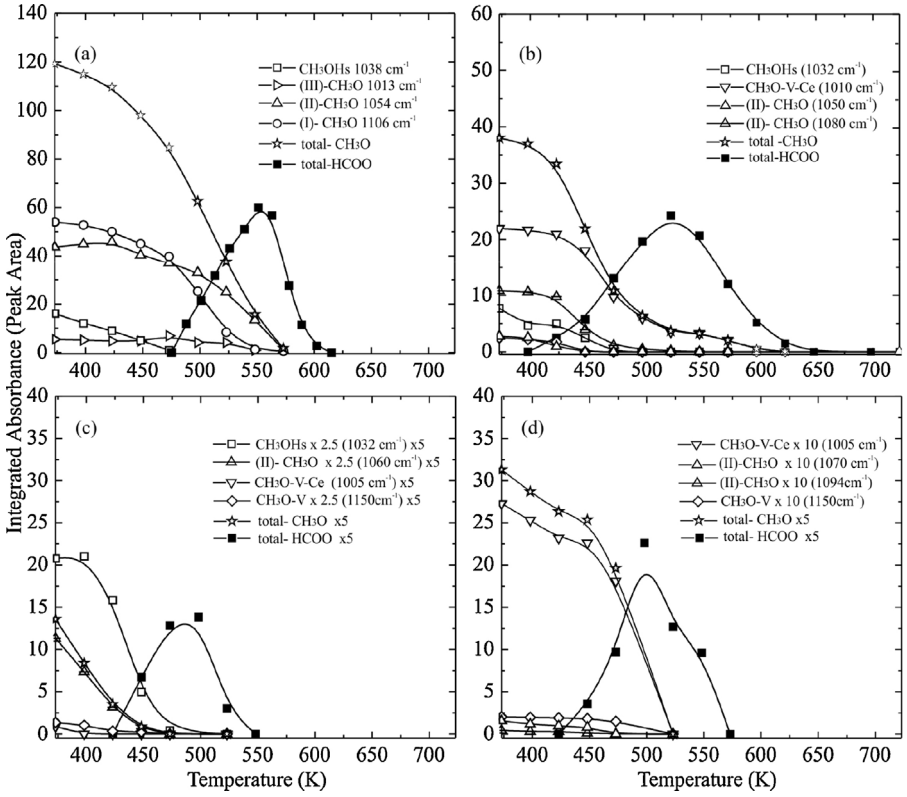

Fig. 9. Evolution of the integrated intensity of IR characteristic bands of surface species during the TPSR of adsorbed methanol: (a) CeO2, (b) 2VCe, (c) 5VCe and (d) CeVO4.

It was proposed that the interaction between VO_x species supported on ceria is due to the formation of V-O-Ce interfacial sites ($CeVO_4$). As was stated before, previous reports showed that the vanadia-ceria interaction renders vanadia sites unreducible, stabilizing its 5+ valence in vanadium and 3+ in ceria at the interface [19,39]. Thus, it can be proposed that the redox cycle would occur on the ceria sites next to vanadia [15,19,67]. Under this picture, V–O–Ce sites could be the active site for the methanol surface reaction, but reactivity would be bound to the support cation rather than to the supported cation. Then, the higher reactivity of 5VCe could be due to the presence of a higher amount of active V–O–Ce interfacial sites, and thus interface ceria sites. This observation was also made from Abbott [4] and Ganduglia-Pirovano [12]. Wherein assume that the mayor reactivity at minor temperature is due to the reactivity of essentially monomeric V=O species surrounded by a reduced ceria surface, and that reduction of the ceria support is the key factor determining the superior activity of ceria supported vanadia catalysts, that is, V–O–Ce interphase sites.

To explain the oxidation of methoxy species adsorbed on VO_x/CeO_2(1 1 1), Kropp et al. [10] investigated the transfer of hydrogen from the CH_3O moiety to: (i) the vanadyl (V=O), (ii) to the oxygen site on the support (Ce–O) and (iii) to the oxygen at the V–O–Ce interphase. They found that the pathway with the lower activation energy was the one where hydrogen is transferred to V–O–Ce, forming a OH. In this case, the methoxy was adsorbed on a Ce^{3+} site (vacancy site). We have observed that signals from OH groups increased during the TPSR in the vanadia-ceria catalyst (Figs. 7 and 8). Thus, under this frame, the most favorable abstraction of hydrogen by the V–O–Ce interphase sites could be the reason of the higher reactivity of this catalytic system as compared with pure ceria.

5. Conclusions

Combination of Raman spectroscopy and methanol adsorption and surface reaction followed by in situ FTIR spectroscopy allowed characterizing the surface structure and reactivity of ceria-supported vanadia catalysts, using pure CeO_2 and $CeVO_4$ samples as reference materials. The surface of the vanadia supported catalyst presented a heterogeneous structure composed of VO_x, $CeVO_4$ and a precursor of the later. Mostly Ce^{3+} is present on the catalysts, which is revealed by the distribution of the methoxy groups. This is a direct evidence of the reductive solid reaction of VO_x species with the ceria surface, even under oxidizing treatment. The reactivity to decompose adsorbed methanol/methoxy species indicates a synergic effect due to the interaction of vanadia with the support. We conclude that the reactivity is related to the special interphase sites, Ce–O–V, which could favor the transfer of hydrogen during the methoxy transformation to formates groups and, finally, carbonate/carbon dioxide.

Acknowledgments

The authors acknowledge the financial support of the National Agency for Scientific and Technological Promotion (projects PICT-2012-1280, PICT-2010-0836 and PME 311/06), the Universidad Nacional del Litoral (grants CAI+D 2011 PI 50120110100311 and 50120110100100) and Spanish Ministry (grant CTQ2011- 25517-E).

Appendix A. Supplementary data

Supplementary data associated with this article can be found, in the online version, at http://dx.doi.org/10.1016/j.molcata.2015.07.012

References

[1] M. Badlani, I.E. Wachs, Catal. Lett. 75 (2001) 137–149.
[2] Khatib S.J., Catalizadores de óxidos de metales de transición (Mo, V, Cr) soportados en γ-alúmina para deshidrogenación oxidativa de propano, Universidad Autónoma de Madrid, Facultad de Ciencias; Instituto de Catálisis y Petroquímica (CSIC), 2007.
[3] L.J. Burcham, L.E. Briand, I.E. Wachs, Langmuir 17 (2001) 6164–6174.
[4] H.L. Abbott, A. Uhl, M. Baron, Y. Lei, R.J. Meyer, D.J. Stacchiola, O. Bondarchuk, S. Shaikhutdinov, H.J. Freund, J. Catal. 272 (2010) 82–91.
[5] Y. Li, Z. Wei, J. Sun, F. Gao, C.H.F. Peden, Y. Wang, J. Phys. Chem. C 572 (2013) 2–572.
[6] G.S. Wong, M.R. Concepcion, J.M. Vohs, J. Phys. Chem. C 106 (2002) 6451–6455.
[7] I.E. Wachs, Dalton Trans. 42 (2013) 11762–11769.
[8] C. Popa, M.V. Ganduglia-Pirovano, J. Sauer, J. Phys. Chem. C. 115 (2011) 7399–24142.
[9] L.J. Burcham, G. Deo, X. Gao, I.E. Wachs, Top. Catal. 11-12 (2000) 85–100.
[10] T. Kropp, J. Paier, J. Sauer, J. Am. Chem. Soc. 136 (2014) 14616–14625.
[11] J. Paier, T. Kropp, C. Penschke, J. Sauer, Faraday Discuss. 162 (2013) 233–245.
[12] M.V. Ganduglia-Pirovano, C. Popa, J. Sauer, H. Abbott, A. Uhl, M. Baron, D. Stacchiola, O. Bondarchuk, S. Shaikhutdinov, H.J. Freund, J. Am. Chem. Soc. 132 (2010) 2345–2349.
[13] R.L. Frost, K.L. Erickson, M.L. Weier, O. Carmody, Spectrochim. Acta A 61 (2005) 829–834.
[14] M.A. Bañares, I.E. Wachs, J. Raman Spectrosc. 33 (2002) 359–380.
[15] M.V. Martínez-Huerta, G. Deo, J.L.G. Fierro, M.A. Bañares, J. Phys. Chem. C 111 (2007) 18708–18714.
[16] S.E. Collins, M.A. Baltanás, A.L. Bonivardi, Appl. Catal. A 295 (2005) 126–133.
[17] E. Finocchio, M. Daturi, C. Binet, J.C. Lavalley, G. Blanchard, Catal. Today 52 (1999) 53–63.
[18] C. Binet, A. Badri and J.-C. Lavalley, J. Phys. Chem. 98 (1994) 6392-6398.
[19] M.A. Bañares, M. Martínez-Huerta, X. Gao, I.E. Wachs, J.L.G. Fierro, Stud. Surf. Sci. Catal. 130 (2000) 3125–3130.
[20] S.E. Collins, L.E. Briand, L.A. Gambaro, M.A. Baltanás, A.L. Bonivardi, J. Phys. Chem. C 112 (2008) 14988–15000.
[21] S. Collins, G. Finos, R. Alcántara, E. del Rio, S. Bernal, A. Bonivardi, Appl. Catal. A 388 (2010) 202–210.
[22] W.H. Weber, K.C. Hass, J.R. McBride, Phys. Rev. B 48 (1993) 178–185.
[23] Z. Wu, M. Li, J. Howe, H.M. Meyer, S.H. Overbury, Langmuir 26 (2010) 16595–16606.
[24] U. Opara Krasovec, B. Orel, A. Surca, R. Reisfeld, Sol. State Ionics 118 (1999) 195–214.
[25] L. Abello, E. Husson, Y. Repelin, G. Lucazeau, Spectrochim. Acta 39 (1983) 641–651.
[26] I.E. Wachs, Catal. Today 27 (1996) 437–455.
[27] S. Xie, E. Iglesia, A.T. Bell, J. Phys. Chem. B 105 (2001) 5144–5152.
[28] T.R. Gilson, O.F. Bizri, N. Cheetham, J. Chem. Soc. Dalt. Trans. (1973) 291–294.
[29] A.E. Lewandowska, M. Calatayud, F. Tielens, M.A. Bañares, J. Phys. Chem. C 115 (2011) 24133–24142.
[30] L.E. Briand, W.E. Farneth, I.E. Wachs, Catal. Today 62 (2000) 219–229.
[31] J.M. Tatibouët, Appl. Catal. A 148 (1997) 213–252.
[32] I.E. Wachs, J.-M. Jehng, W. Ueda, J. Phys. Chem. B 109 (2005) 2275–2284.
[33] J. Castillo-Charaí, E.L. Sibert, J. Chem. Phys. 119 (2003) 11671–11681.
[34] M.P. Andersson, P. Uvdal, a. D. MacKerell, J. Phys. Chem. B 106 (2002) 5200–5211.
[35] L.J. Burcham, L.E. Briand, I.E. Wachs, Langmuir 17 (2001) 6175–6184.
[36] L.J. Burcham, M. Badlani, I.E. Wachs, J. Catal. 203 (2001) 104–121.
[37] L.J. Burcham, I.E. Wachs, Catal. Today 49 (1999) 467–484.
[38] G. Cabilla, A.L. Bonivardi, M.A. Baltanás, J. Catal. 201 (2001) 213–220.
[39] M. Baron, H. Abbott, O. Bondarchuk, D. Stacchiola, A. Uhl, S. Shaikhutdinov, H.J. Freund, C. Popa, M.V. Ganduglia- Pirovano, J. Sauer, Angew. Chem. Int. Ed. 48 (2009) 8006–8009.
[40] E.J. Baran, M.E. Escobar, Spectrochim. Acta. 41 (1985) 415–417.
[41] P. Boulet, A. Baiker, H. Chermette, F. Gilardoni, J. Volta, J. Weber, J. Phys. Chem. B 106 (2002) 9659–9667.
[42] I.E. Wachs, Catal. Today 100 (2005) 79–94.
[43] E.J. Baran, P. Aymonino, Z. Anorg, Allg. Chem. 383 (1971) 220–225.
[44] C. Li, K. Domen, K. Maruya, T. Onishi, J. Catal. 125 (1990) 445–455.
[45] A. Badri, C. Binet, J. Lavalley, J. Chem. Soc. 93 (1997) 1159–1168.
[46] J. Lamotte, V. Morávek, M. Bensitel, J.C. Lavalley, React. Kinet. Catal. Lett. 36 (1988) 113–118.
[47] C. Binet, M. Daturi, Catal. Today 70 (2001) 155–167.
[48] S. Collins, M. Baltanas, A.L. Bonivardi, J. Catal. 226 (2004) 410–421.
[49] Z. Wu, M. Li, D.R. Mullins, S.H. Overbury, ACS Catal. 2 (2012) 2224–2234.
[50] S. Rousseau, O. Marie, P. Bazin, M. Daturi, S. Verdier, V. Harlé, J. Am. Chem. Soc. 132 (2010) 10832–10841.
[51] P. Bazin, S. Thomas, O. Marie, M. Daturi, Catal. Today 182 (2012) 3–11.
[52] G. Busca, J. Mol. Catal. 50 (1989) 241–249.
[53] G.N. Vayssilov, M. Mihaylov, P. St Petkov, K.I. Hadjiivanov, K.M. Neyman, J. Phys. Chem. B 115 (2011) 23435–23454.
[54] G. Busca, V. Lorenzelli, Mater. Chem. 7 (1982) 89–126.
[55] P.G. Gopal, R.L. Schneider, K.L. Watters, J. Catal. 105 (1987) 366–372.
[56] W.O. Gordon, Y. Xu, D.R. Mullins, S.H. Overbury, Phys. Chem. Chem. Phys. 11 (2009) 11171–11183.

[57] C. Binet, M. Daturi, J. Lavalley, Catal. Today 50 (1999) 207–225.
[58] C. Binet, A. Badri, M. Boutonnet-Kizling, J. Lavalley, J. Chem. Soc., Faraday Trans. 90 (1994) 1023–1028.
[59] M. Li, Z. Wu, S.H. Overbury, J. Catal. 306 (2013) 164–176.
[60] C. Binet, M. Daturi, J.-C. Lavalley, Catal. Today. 50 (1999) 207–225.
[61] K. Nakamoto, Infrared and Raman Spectra of Inorganic and Coordination Compounds, Ed, Wiley, New York, 1996.
[62] S.E. Collins, M.A. Baltanás, A.L. Bonivardi, J. Phys. Chem. B 110 (2006) 5498–5507.
[63] C. Morterra, G. Magnacca, Catal. Today 27 (1996) 497–532.
[64] F. Ouyang, A. Nakayama, K. Tabada, E. Suzuki, J. Phys. Chem. B 104 (2012) 2012–2018.
[65] M.J. Vecchietti, S. Collins, W. Xu, L. Barrio, D. Stacchiola, M. Calatayud, F. Tielens, J.J. Delgado, A. Bonivardi, J. Phys. Chem. C 117 (2013) 8822–8831.
[66] M.V. Martínez-Huerta, G. Deo, J.L.G. Fierro, M.A. Bañares, J. Phys. Chem. C 112 (2008) 11441–11447.
[67] M.V. Martinez-Huerta, J.M. Coronado, M. Fernández- García, A. Iglesias-Juez, G. Deo, J.L.G. Fierro, M.A. Bañares, J. Catal. 225 (2004) 240–248.